Heliyon 9 (2023) e17101

Contents lists available at ScienceDirect

Heliyon

journal homepage: www.cell.com/heliyon

Identification of the prognostic biomarkers and their correlations with immune infiltration in colorectal cancer through bioinformatics analysis and *in vitro* experiments

Min Guo [a,1], Xiaxi Li [b,1], Jiong Li [c], Baolong Li [d,*]

[a] *Department of Oncology, The Fifth Affiliated Hospital, Southern Medical University, Guangzhou, Guangdong, China*
[b] *Department of Gastroenterology, Shenzhen Hospital, Southern Medical University, Shenzhen, Guangdong, China*
[c] *Department of Anatomy, Neuroscience Laboratory for Cognitive and Developmental Disorders, Medical College of Jinan University, Guangzhou, Guangdong, China*
[d] *Department of General Surgery, The Fifth Affiliated Hospital, Southern Medical University, Guangzhou, Guangdong, China*

ARTICLE INFO

Keywords:
Colorectal cancer (CRC)
Hub gene
Prognosis
Immune infiltration
BIRC5

ABSTRACT

Colorectal cancer (CRC) is the third most diagnosed malignancy and the second leading cause of cancer death. The objective was to identify novel hub genes that were helpful for prognosis and targeted therapy in CRC. GSE23878, GSE24514, GSE41657, GSE81582 were filtered from the gene expression omnibus (GEO). Differentially expressed genes (DEGs) were identified through GEO2R, which were enriched in the GO term and KEGG pathway in DAVID. PPI network was constructed and analyzed using STRING and hub genes were screened out. The relationships between hub genes and prognoses in CRC were evaluated in GEPIA based on the cancer genome atlas (TCGA) and genotype-tissue expression (GTEx). The transcription factors and miRNA-mRNA interaction networks for hub genes were performed using miRnet and miRTarBase. The relationship between hub genes and tumor-infiltrating lymphocytes were analyzed in TIMER. The protein levels of hub genes were identified in HPA. The expression levels of hub gene in CRC and its effect on the biological effect of CRC cells were identified *in vitro*. As hub genes, the mRNA levels of BIRC5, CCNB1, KIF20A, NCAPG, and TPX2 were highly expressed in CRC and had excellent prognostic value. The BIRC5, CCNB1, KIF20A, NCAPG, and TPX2 were closely associated with transcription factors, miRNAs, tumor-infiltrating lymphocytes, suggesting their involvement in the regulation of CRC. BIRC5 highly expressed in CRC tissues and cells, and promoted the proliferation, migration, and invasion of CRC cells. BIRC5, CCNB1, KIF20A, NCAPG, and TPX2 are hub genes that serve as promising prognostic biomarkers in CRC. BIRC5 plays an important role in the development and progression of CRC.

1. Introduction

Globally, colorectal cancer (CRC) is the third most diagnosed malignancy and the second leading cause of cancer deaths [1]. In

* Corresponding author. Department of General surgery, The Fifth Affiliated Hospital, Southern Medical University, Guangzhou, 510900, Guangdong, China.
E-mail addresses: libaolong1457@163.com, ptwk141@smu.edu.cn (B. Li).
[1] The authors contributed equal to this work.

https://doi.org/10.1016/j.heliyon.2023.e17101
Received 7 November 2022; Received in revised form 6 June 2023; Accepted 7 June 2023
Available online 12 June 2023

2020, there were 147,950 individuals diagnosed with CRC in the United States, including 104,610 cases of colon cancer and 43,340 cases of rectal cancer. An estimated 53,200 individuals (35.6%) were projected to die from the CRC [2]. In other high-income of countries such as Italy, Norway, and Spain, the incidences of CRC are increasing whilst some economically transitioning countries like China, Brazil, and Slovakia are experiencing increasing incidences [3]. In several countries such as Spain, Poland, and Latvia, the mortality rates of CRC plateaued after the start of the heterogeneous screening programs, although CRC incidence rates continued to increase [4]. Nowadays, genetic predisposition has been a risk factor for CRC [5].

A comprehensive understanding of the etiology, epidemiology, and molecular biology of CRC will contribute to early diagnosis and precise therapy in patients. Recent research has revealed that T cell checkpoint inhibitor treatment targeting programmed cell death-1 (PD-1), programmed cell death ligand-1 (PD-L1), T cell immunoglobulin mucin receptor 3 (TIM3), and lymphocyte activation gene 3 protein (LAG3) are potentially efficacious against CRC and had tolerable safety levels in preclinical and clinical trials [6]. The large-scale genomic analysis of CRC suggested that microsatellite instability (MSI)-high CRC patients frequently undergo immunoediting which allowed CRC immune escape despite frequent lymphocytic infiltration and high mutational load. In addition, CRC has genetic and methylation events that are related to activated WNT signaling and T-cell exclusion [7]. The recent research has demonstrated that circulating tumor DNA (ctDNA) can, in principle, be easily incorporated into the conventional follow-up to complement modalities such as carcinoembryonic antigen (CEA) test and radiographic imaging, to help stratify CRC patients' risk for recurrence [8]. The microRNA (miRNA) study showed that CRC resistance to cetuximab was mediated by up regulation of the miR-100 and miR-125 b [9]. However, early diagnosis and precise therapy of CRC is still a great challenge.

Our study aims to offer a comprehensive understanding of the etiopathogenesis of CRC and verify the new biomarkers for prognosis and targeted therapy of CRC. Microarray technology can contribute to monitoring the alteration of gene expression during the genesis and progression of cancer. However, it is very hard to obtain conclusive results from a single microarray analysis. In our study, four gene expression profiles (GSE23878, GSE24514, GSE41657, GSE81582) were combined, for the first time, for integrative bioinformatics analysis in the gene expression omnibus (GEO). All the differentially expressed genes (DEGs) were identified in CRC tissues versus normal colorectal tissues. Gene ontology (GO) and kyoto encyclopedia of genes and genomes (KEGG) pathway of DEGs were performed to explored the function of DEGs. The protein-protein interaction (PPI) network was constructed to identify the hub genes through the search tool for the retrieval interacting genes (STRING) database. The expression and prognostic value of the hub genes in CRC were verified in the gene expression profiling interactive analysis (GEPIA) platform. The correlation between hub genes and transcription factors, miRNAs, immune infiltration were explored in miRnet, miRTarBase, tumor immune estimation resource (TIMER) databases, respectively. The protein levels of hub genes were identified in the human protein atlas (HPA). Then, the expression levels of hub gene BIRC5 in CRC and its effect on the biological effect of CRC cells were verified *in vitro*, revealing it can be a promising biomarker and potential therapeutic target for CRC.

2. Material and methods

2.1. Data extraction

The four gene expression profiles (GSE23878, GSE24514, GSE41657, and GSE81582) were acquired from the GEO (https://www.ncbi.nlm.nih.gov/geo). The GEO database is used for storing the sequence and array data. The GSE23878 included 35 CRC samples and 24 normal colorectal samples [10]. The GSE24514 covered 34 CRC samples and 15 normal samples [11]. The GSE41657 contained 25 CRC samples and 12 normal colorectal samples. GSE81582 included of 42 CRC samples and 9 normal colorectal samples [12].

2.2. Data processing

The online tool-GEO2R (https://www.ncbi.nlm.nih.gov/gov/geo/geo2r) was used for screening the DEGs from the gene expression profiles **(GSE23878, GSE24514, GSE41657, and GSE81582)** between the CRC samples and normal samples, respectively. The adjusted *P*-value (adjust P) < 0.05 and $|\log_2$ Fold Change ($\log_2$ FC) $|> 1$ were applied to identify DEGs.

2.3. GO and KEGG pathway analysis of DEGs

The GO and KEGG pathways of DEGs were analyzed in the database for annotation, visualization, and integrated discovery (DAVID version 6.8 https://david.ncifcrf.gov/tools.jsp) [13,14]. The GO terms included biological process, cellular components, molecular function. Background: *Homo sapiens*. $P < 0.05$ was set as the threshold criterion.

2.4. Analysis of PPI network

The function interaction of DEGs was analyzed in the STRING (version 11.0 https://string-db.org) The STRING database aims to collect and integrate information by consolidating known and predicted protein-protein interaction data for a large number of organisms. The interactions in STRING database include direct (physical) interactions, as well as indirect (functional) interactions, as long as both are specific and biologically meaningful [15]. The score of confidence >0.9 was viewed as statistically significant (the highest confidence). The Cytoscape (version 3.7.1) was used to perform the PPI network analysis. The parameter settings were: degree cut off = 2, node score off = 2, maximum depth = 100, and k-score = 2 [16]. The genes with the degree >10 were identified as the hub genes. The significant module was filtered by molecular complex detection (MCODE).

2.5. Survival analysis and validation of hub genes

The mRNA expression levels and overall survival rates of hub genes were analyzed by using the GEPIA platform (http://gepia.cancer-pku.cn) which is an online resource for analyzing the data from the cancer genome atlas (TCGA) and genotype-tissue expression (GTEx) database [17]. The clinical data of CRC patients were divided into two groups based on the transcripts per million (TPM) of hub genes. The high group was one with the TPM higher than the upper quartile. The low group included those with TPM lower than the lower quartile. The log-rank $P < 0.05$ and P (HR) < 0.05 were set as the threshold criteria.

2.6. Analysis of TF and miRNA-mRNA regulate network for hub genes

The miRnet (version 2.0 https://www.mirnet.ca/) can be used to search the transcription factors (TFs) for genes, which are based on TRRUST, RegNetwork, ENCODE, JASPER, and ChEA [18]. The miRTarBase (version 8.0 http://mirtarbase.cuhk.edu.cn) contains more than 360,000 miRNA-target interactions, which are verified experimentally by reporter assay, Western blot, qPCR, microarray, and next-generation sequencing experiments [19]. The transcription factors and microRNAs for the potential prognostic hub genes were filtered from the miRnet and the miRTarBase. The Cytoscape (version 3.7.1) was applied to construct TFs and miRNA-mRNA networks. The tissue type was intestinal tissue.

2.7. Immune cells infiltration analysis of hub genes

TIMER (https://cistrome.shinyapps.io/timer) is the webserver for analyzing the immune cell infiltrates across the various kinds of cancers from the TCGA [20]. TIMER was utilized to analyze the correlation between the infiltrating immune cells and hub genes in colon adenocarcinoma (COAD) and rectum adenocarcinoma (READ) using the deconvolution method, respectively. The $P < 0.05$ was set as the threshold criterion.

2.8. Immunohistochemical analysis of hub genes

The protein levels of the potential prognostic hub genes in CRC samples and normal colorectal samples were obtained from the HPA (version 20.0 https://www.proteinatlas.org/), which contained immunohistochemical expression data for human samples [21]. The protein levels were divided into four groups: high, medium, low, and not detected through the scoring system, which contained the proportion of staining cells (>75%, 75%–25%, and <25%) and intensity of stain (strong, moderate, weak and negative). Hub gene whose expression trend was consistent with GEO was screened for subsequent analysis.

2.9. Tissues and cells

The 30 paired CRC tissues and adjacent normal tissues were obtained from the fifth affiliated hospital of Southern Medical University. All participating patients provided informed consent and signed informed consent forms. HCT116 and SW480 cell lines were purchase form the Cell Bank of the Shanghai Chinese Academy of Sciences (Shanghai, China). Cells were maintained in DMEM containing 10% FBS and 1% penicillin/streptomycin solution. Cells were cultivated in a humidified incubator with 5% CO_2 under normoxic conditions at 37 °C.

2.10. Quantitative real-time PCR

First, total RNA was isolated from CRC tissues and adjacent normal tissues by Trizol Reagent (Life Technologies, Guilford, CT), and the quantity and quality of total RNA was detected using a Nanodrop ND-1000 (NanoDrop Technologies, Wilmington, DE), total RNA integrity was assessed by agarose gel electrophoresis. Samples were accepted and used for cDNA synthesis in according with the A260/280 ratio lies between 1.8 and 2.0. Second, cDNA was synthesized from 1 μg RNA using a universal cDNA synthesis kit (TRANS, Beijing, China). Immediately after, A SYBR Green-based qPCR (Yeasen, Shanghai, China) assay was performed using human GAPDH- and BIRC5-specific primers. The sequences of primers used were included. GAPDH, forward: 5′-TGTTGCCATCAATGACCCCTT-3'; and GAPDH, reverse: 5′-CTCCACGACGTACTCAGCG-3'; BIRC5, forward: 5′-TTGTCTAAGTGCAACCGCCT-3'; and BIRC5, reverse: 5′-CACAACCCTTCCCAGACTCC-3'; Third, the PCR products were analyzed in a melting curve analysis to verify the presence of a gene-specific qRT-PCR product and qRT-PCR products were also confirmed for one specific size band by agarose gel electrophoresis. Finally, all quantifications of the target mRNA was normalised using GAPDH mRNA as a reference gene. Relative mRNA quantization was performed according to the $2^{-\triangle\triangle CT}$ method.

2.11. Immunohistochemical

For immunohistochemical (IHC) stainings, fixed in 4% paraformaldehyde for 30 min at room temperature or overnight at 4 °C, pelleted, and embedded in paraffin blocks. Paraffin-embedded samples were serially sectioned at 4 μm thickness. Antigen retrieval was performed by a pressure cooker for 30 min in 0.01 M citrate buffer (pH 6.0), followed by treatment with 3% hydrogen peroxide for 5 min. Specimens were incubated with monoclonal antibodies against human BIRC5 (1:500, ab134170, abcam, USA) overnight at 4 °C. Immunostaining was performed using DAB or Permanent Red (Dako) according to the manufacturer's instructions. IHC overview

images were taken using a CL 1500 ECO stereomicroscope (Carl Zeiss, Oberkochen, Germany) and a ToupCam camera (UCMOS, ToupTek Photonics, China).

2.12. Western blotting

Western blotting was performed using standard methods. The equal amounts of protein per sample were separated by 10% SDS-PAGE and then transferred to PVDF membrane (0.2 μm pore size, Millipore), and after 1 h of exposure to 5% non-fat milk in TBST (150 mM NaCl, 20 Mm Tris, pH 7.5, 0.1% Tween-20) to block nonspecific binding. After doing so, we incubated primary antibodies: mouse *anti*-BIRC5/Survivin (1:2000, TA502234, Thermo Fisher, USA), GAPDH (1:2000, AF0006, Biyuntian Biological Co., Ltd. China) overnight at 4 °C. Next, the membranes were incubated with horseradish peroxidase (HRP)-conjugated anti-mouse (1:5000, AS014, ABclonal, China) secondary antibody. Immunoreactive proteins were visualized by using the ECL detection system (GE Healthcare Bio-Sciences).

2.12.1. CCK8 assays

For CCK8 assay, the Cell Couting Kit-8 (CCK8, Dojindo, Shanghai, China) was used following the produceers suggestions. Brifely, cells were seeded in 96-well plates at a density of 2×10^3 cells/well, and 10 μL of CCK8 solution was added to each well (100 μL medium). After incubation at 37 °C with 5% CO_2 for 4 h, the plates were measured at 450 nm with a microplate reader to determine the proliferative ability of colorectal cancer cells.

2.13. Transwell assays

Transwell assays were divided into migration and invasion assays. The basic operation was as follows: HCT116 and SW480 cell density were adjusted to 1×10^5 cells/well and seeded into the upper chamber in serum-free medium. Then, 500 μL DMEM containing 10% FBS were added to the lower chamber. Fifty microliters of matrigel was added in the upper chamber when performing transwell invasion assay. Cells in the upper chamber were removed with cotton and the migrated cells were stained with 0.1% crystal violet solution (Solarbio, China) and captured using a microscope (200 ×, Leica DMIRB microscope) in ten random fields.

2.14. Statistical analysis

Statistical analyses were performed by using GraphPad Prism Software (GraphPad Prism version 8.3.1, www.graphpad.com). All quantitative date in this study were presented as means ± SEM. Two-tailed Student's t-test or one-way ANOVA followed by Turkey's test as the post-hoc test. $P < 0.05$ indicated as statistically significant.

3. Results

3.1. Identification of DEGs in CRC

A total of 2380, 758, 3670, and 2115 DEGs were screened from the GSE23878, GSE24514, GSE41657, and GSE81582, respectively. 281 DEGs were consistently expressed in the four gene datasets (Fig. 1A and B). They covered 102 up-regulated and 179 down-

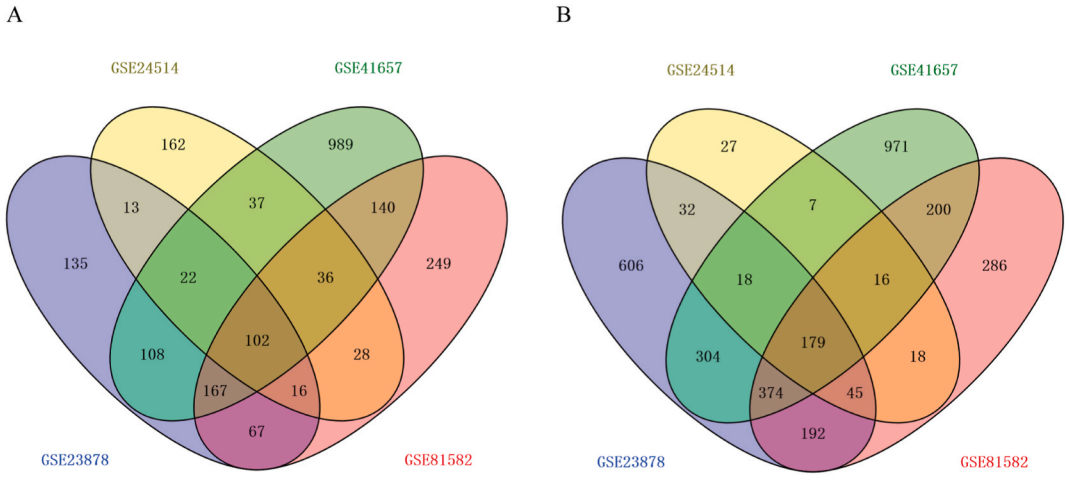

Fig. 1. Identification of differentially expressed genes (DEGs) between CRC tissues and normal colorectal tissues in the four-gene expression profiles. (A). 102 up-regulated genes had the log2 FC > 1 and adjusted $P < 0.05$. (B). 179 down-regulated genes had the log2 FC < −1 and adjusted $P < 0.05$.

regulated DEGs (Table 1).

3.2. GO and KEGG pathway analysis of DEGs

In the GO term and KEGG pathway, the DEGs were divided into four groups: the biological process, cellular components, molecular function, and the KEGG pathway groups. Top 5 GO terms and KEGG pathways were screened out according to the gene counts for up-regulated DEGs and down-regulated DEGs (Fig. 2A and B).

3.3. PPI network and module analysis of DEGs

The 107 genes out of the 281 DEGs were filtered to construct the PPI network. The PPI network contained 107 nodes and 417 sides. It included 56 up-regulated and 51 down-regulated genes (Fig. 3A). In total, 27 genes, whose degree >10, were identified as the hub genes (Table 1 is bold). The characteristics of hub genes were shown in Table 2. The significant module was selected from the PPI network through the MCODE module (Fig. 3B).

3.4. Survival analysis and validation of hub genes in CRC

The survival analysis curve of CRC patients in the TCGA was performed using the GEPIA based on the mRNA expression levels of hub genes. The results showed that the high expression levels of BIRC5, CCNB1, KIF20A, NCAPG, TPX2 were associated with the higher percents of overall survival in CRC patients (Fig. 4A–E). The dotted lines represented 95% confidence interval of survival rates. In summary, the BIRC5, CCNB1, KIF20A, NCAPG, and TPX2 were considered as the hub genes with good prognostic value. The GEPIA was applied for analyzing the mRNA expression of BIRC5, CCNB1, KIF20A, NCAPG, and TPX2 in TCGA and GTEx (colon adenocarcinoma samples VS normal samples, rectum adenocarcinoma VS normal samples). The trend of prognostic hub genes was the same as in the GEO (Fig. 5A–E).

3.5. TFs-mRNA and miRNA-mRNA regulatory network analysis for prognostic hub genes

The TFs for the prognostic hub genes (BIRC5, CCNB1, KIF20A, NCAPG, and TPX2) were predicted using the miRNet. The TFs regulatory network included 2 hub genes and 35 TFs (Fig. 6A). The interaction between the above prognostic hub genes and microRNAs was predicted based on the reporter assay in miRTarBase. The miRNA-mRNA consisted of 3 hub genes and 12 microRNAs (Fig. 6B).

3.6. Immune infiltrate analysis for prognostic hub genes

The relationship between the mRNA expression of BIRC5, CCNB1, KIF20A, NCAPG, TPX2, and immune cells in CRC was analyzed in the TIMER (Fig. 7A–J).

In colon adenocarcinoma, BIRC5 demonstrated a significant correlation with the abundance of neutrophils; CCNB1 demonstrated significant correlations with the abundance of B cells, $CD8^+$ T cells, $CD4^+$ T cells, neutrophils, and dendritic cells; KIF20A demonstrated significant correlations with the abundance of B cells, $CD8^+$ T cells, $CD4^+$ T cells, neutrophils, and dendritic cells; NCAPG demonstrated significant correlations with the abundance of B cells, $CD8^+$ T cells, neutrophils, and dendritic cells; TPX2 demonstrated significant correlations with the abundance of $CD4^+$ T cells, and macrophages.

Table 1
DEGs in CRC tissues compared with normal tissues.

DEGs	Gene Name
Up-regulated	CDH3, CEMIP, HILPDA, GTF2IRD1, SOX4, INHBA, SLCO4A1, TEAD4, NFE2L3, PUS7, TGFBI, MRGBP, SLC52A2, MMP7, CENPN, MMP11, CSE1L, TESC, TRIP13, **NEK2**, **MCM2**, CDC25B, **CDC20**, XPOT, SHMT2, **BIRC5**, CCND1, AHCY, SLC7A5, ADGRG1, GDF15, **KIF20A**, GINS1, PSAT1, CDK4, **AURKA**, PUS1, CHI3L1, MET, S100A11, F12, **TPX2**, PAFAH1B3, TRIM29, TMEM97, **MCM7**, SORD, SCDUBE2S, NT5DC2, HMGA1, COL11A1, ECT2, **MCM4**, **KIF2C**, **KIF4A**, **MELK**, DHCR7, **CDK1**, **BUB1**, GART, FANCI, CAD, TIMP1, SLC7A11, DTL, ARNTL2, KLK10, MRPS17, **TTK**, **CEP55**, SOX9, **RRM2**, NEBL, FEN1, SLC7A1, **PRC1**, **CENPF**, **BUB1B**, CKS2, **TOP2A**, **CKAP2**, COL1A1, **MKI67**, FXYD5, **CXCL1**, **CCNB1**, **NCAPG**, TACSTD2, VSNL1, GINS2, ENC1, CXCL3, CXCL8, SERPINB5, LY6E, **ASPM**, PHLDA1, SLCO1B3, FERMT1, LGR5, CXCL2.
Down-regulated	ABCA8, BCHE, CA7, CXCL12, TSPAN7, SST, ATP1A2, ADH1B, SFRP1, CFD, LPAR1, SDPR, SGK1, NR3C2, CHRDL1, PYY, PLPP1, IL6R, GUCA2B, SPARCL1, METTL7A, FGL2, FAM107A, STMN2, GPM6B, GCG, MFAP4, PLN, ADTRP, ADAMTSL3, VIP, SETBP1, NAAA, MYH11, ADAMDEC1, ARL14, SLC4A4, CHGA, DHRS11, KLF4, ADH1C AKR1B10, PTGER4, CPM, HPGD, AOC3, CHP2, KCNMA1, CCL19, PDE9A, MT1M, PRKCB, ENTPD5, MYLK, GUCA2A, PDK4, ZBTB16, IGHM, SRI, FNBP1, SMPDL3A, PBLD, SYNM, LGALS2, NEDD4L, FAM129A, PPP1R12 B, MAOA, CNN1, CBX7, SLC26A2, DCN, FGFR2, SLC17A4, ITIH5, RCAN1, LMO3, HAND2-AS1, BEST2, HIGD1A, EML1 EDN3, RGS2, AHNAK, CAV1, DES, PTGS1, HHLA2, FUCA1, FOXF2, FOXN3, HSD17B2, CA2, ACTG2, SGCE, KCNMB1, TUBAL3, BCAS1, ZG16, PCK1, RETSAT, GPD1L, AQP8, PAPSS2, LRRC19, PHLPP2, BTNL3, JAM3, UGP2, GSN, PDLIM3, SEPP1, NDN, FBLN1, ABCG2, HSD11B2, MYO1A, COX7A1, CLCA1, CA1, CLIC5, SLC26A3, ALDH1A1, EMP1, GDPD3, PADI2, BTNL8, ACAA2, CA4, CD177, PRKACB, PMP22, EPB41L4 B, FCGBP, FERMT2, SCNN1B, ANPEP, CA12, PTPRH, TDP2, PJA2, SELENBP1, VIPR1, ZSCAN18, CLCA4, MS4A12, ITM2C, CDHR5, CSRP1, PLAC8, MEIS1, TAGLN, SLCO2A1, APPL2, MXI1, POU2AF1, JCHAIN, MALL, NPTX1, FAM134B, CES2, C1orf115, MYL9, CEACAM7, NXPE4, MEP1A, KRT20, SGK2, TSPAN1, GPA33, CASQ2, CALD1, CLDN8, AOC1, MUC2, CEACAM1, HSPA2, GCNT3, CKB.

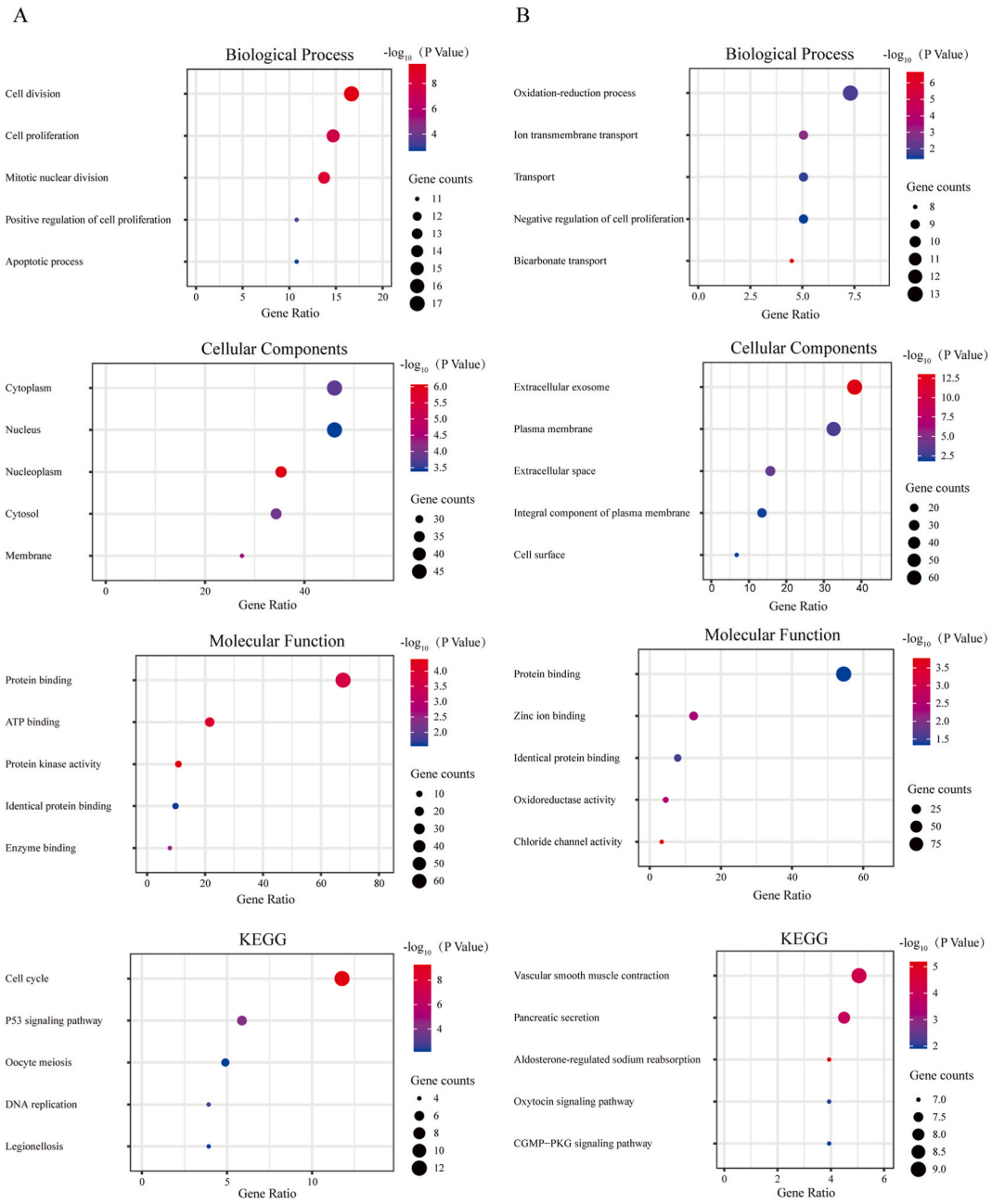

Fig. 2. The Gene Ontology (GO) and Kyoto Encyclopedia of Genes and Genomes (KEGG) pathways of DEGs in the database for annotation, visualization, and integrated discovery (DAVID). (A) GO and KEGG pathway analysis for up-regulated DEGs. (B) GO and KEGG pathway analysis for down-regulated DEGs. The GO term and KEGG pathways were ranked by gene counts. Top 5 GO terms and KEGG pathways were filtered according to gene counts. Gene counts: the number of DEGs enriched genes enriched in each term. Gene Ratio: the ratio of the number of enriched DEGs in each term to the total number of DEGs.

In rectum adenocarcinoma, BIRC5 showed significant correlations with the abundance of macrophages and neutrophils; CCNB1 showed significant correlations with the abundance of neutrophils, $CD8^+$ T cells, $CD4^+$ T cells, and macrophages; KIF20A showed a significant correlation with the abundance of macrophages; NCAPG showed significant correlations with the abundance of $CD8^+$ T cells and neutrophils; TPX2 showed a significant correlation with the abundance of neutrophil. These results suggested that BIRC5, CCNB1, KIF20A, NCAPG and TPX2 played important roles in immune cell infiltration for CRC.

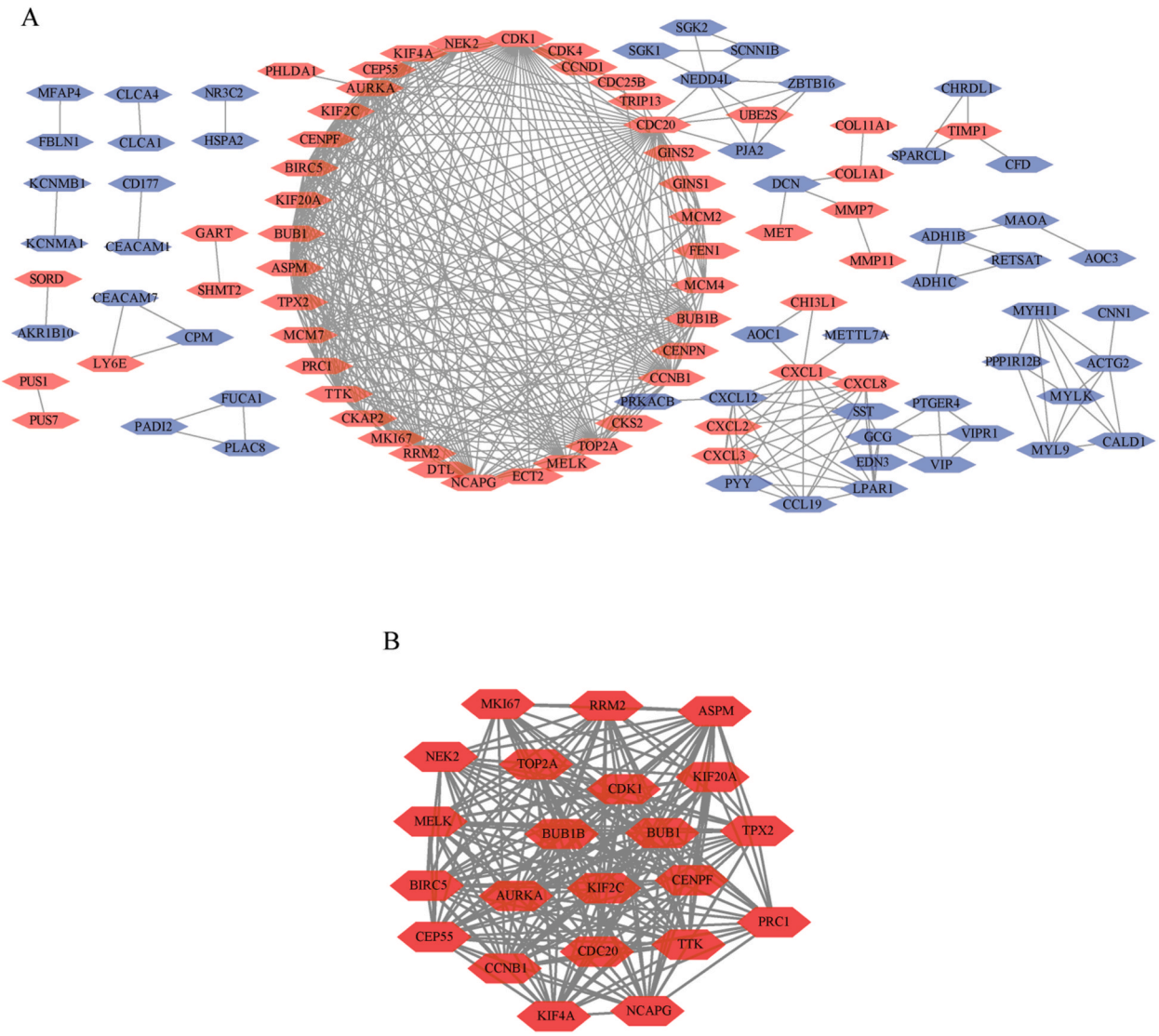

Fig. 3. Protein-protein interaction (PPI) network and significant module of DEGs. (A). The PPI network was composed of 100 nodes and 738 sides. (B). Significant module was filtered from the PPI network through the MCODE. Red nodes represented up-regulated DEGs. Blue nodes represented down-regulated DEGs. The sides represented an interaction relationship between the DEGs.

3.7. Immunohistochemical analysis of prognostic hub genes

In the HPA, the protein expression levels of BIRC5, CCNB1, KIF20A, NCAPG, and TPX2 were identified in an immunohistochemical analysis using the antibodies HPA002830, CAB000115, HPA036909, HPA039613, and HPA005487, respectively (normal colorectal tissues VS CRC tissues). The interpretation results of immunohistochemical staining were provided by HPA. In Fig. 8A–E, these results had confirmed that the protein expression levels of BIRC5, CCNB1, KIF20A, NCAPG, and TPX2 in normal colorectal tissues and CRC tissues. The expression trend of BIRC5 was consistent with the GEO. BIRC5 was screened for subsequent analysis.

3.8. Levels of BIRC5 expression are up-regulated in CRC tissues

We evaluated the expression of BIRC5 in clinical CRC tissues. To this end, we collected 30 paired CRC tissues and adjacent normal tissues and examined the expression of BIRC5 using qRT-PCR. As shown in Fig. 9A, BIRC5 expression was significantly up-regulated in CRC tissues. Consistent with the results of qRT-PCR, the expression levels of BIRC5 in CRC tissues was increased as compared with that in adjacent normal tissues using immunohistochemical (Fig. 9B). Taken together, these observations indicate that BIRC5 levels were up-regulated in CRC tissues.

Table
2The topology characteristics of 27 hub genes.

Gene name	Degree	Averageshortest path length	Betweeness centrality	Closeness centrality	Clustering coefficient	Stress
CDK1	36	1.90	3.02E-01	5.25E-01	4.24E-01	3308
CDC20	35	2.15	2.32E-01	4.66E-01	4.42E-01	1988
CCNB1	30	2.00	2.09E-01	5.00E-01	5.36E-01	2548
TOP2A	27	2.32	1.02E-02	4.31E-01	6.81E-01	338
ASPM	25	2.37	7.29E-03	4.22E-01	7.40E-01	178
BUB1B	25	2.35	8.01E-03	4.25E-01	7.33E-01	204
NCAPG	24	2.37	1.02E-02	4.22E-01	7.03E-01	242
BUB1	24	2.37	3.90E-03	4.22E-01	7.90E-01	156
AURKA	23	2.40	3.80E-02	4.16E-01	7.51E-01	458
RRM2	23	2.39	8.48E-03	4.19E-01	7.27E-01	240
KIF20A	23	2.40	2.08E-03	4.16E-01	8.38E-01	86
BIRC5	22	2.42	2.44E-03	4.13E-01	8.35E-01	82
CENPF	22	2.42	2.02E-03	4.13E-01	8.48E-01	76
KIF2C	22	2.42	1.67E-03	4.13E-01	8.66E-01	66
TTK	22	2.42	2.07E-03	4.13E-01	8.44E-01	78
CEP55	21	2.44	1.14E-03	4.11E-01	8.81E-01	54
MELK	19	2.47	6.95E-04	4.05E-01	9.24E-01	26
TPX2	19	2.47	3.06E-04	4.05E-01	9.47E-01	18
KIF4A	19	2.47	2.71E-04	4.05E-01	9.53E-01	16
PRC1	18	2.47	2.77E-03	4.05E-01	8.04E-01	104
NEK2	16	2.52	5.72E-05	3.97E-01	9.83E-01	4
MKI67	15	2.55	1.92E-04	3.92E-01	9.62E-01	8
MCM4	14	2.55	1.27E-02	3.92E-01	6.48E-01	476
CKAP2	12	2.60	3.58E-04	3.85E-01	9.09E-01	12
CXCL1	11	3.48	9.47E-02	2.87E-01	5.27E-01	658
MCM7	11	2.60	8.90E-03	3.85E-01	6.73E-01	354
MCM2	11	2.60	1.04E-02	3.85E-01	6.18E-01	356

The genes were ranked by degree.

3.9. Down-regulation of BIRC5 suppress proliferation, invasion and migration of CRC cells

Considering that BIRC5 is upregulated in CRC tissues, we cytologically studied the effect of silencing BIRC5 on the behavior of CRC cells *in vitro*. To evaluate the function of the BIRC5 gene in CRC cells, we firstly silenced BIRC5 expression via shBIRC5 lentivirus-infected HCT116 and SW480 cells. LV-shRNA-BIRC5 and LV-shRNA-NC lentivirus was designed and purchased from GeneCopoeia (CSHCTR001-LVRH1GP and HSH009100-LVRH1GP, GeneCopoeia, China). The gene knock down efficiency was confirmed by western blotting (Fig. 10A and B). We next examined whether down-regulation of BIRC5 expression affected the proliferation, migration and invasion of CRC cells. We found that the cell proliferation, migration and invasion abilities were significantly reduced after infection with shBIRC5 lentivirus (Fig. 10C–H). Thus, our results indicated that knockdown of BIRC5 suppressed the proliferation, migration and invasion ability of CRC cells.

4. Discussion

Over the past few decades, the CRC remained one of the most fatal malignant tumors with a poor prognosis in the world [22]. The precise predictive biomarker in CRC would be of great significance to improving the prognosis and choosing the therapeutic options of CRC patients. Therefore, it is very necessary to identify the novel hub genes which can be used as the promising biomarkers for prognosis, and targeted therapy in CRC.

In this research, 102 up-regulated and 179 down-regulated DEGs were identified through the bioinformatic analysis in the four gene datasets (GSE23878, GSE24514, GSE41657, and GSE81582). The GO and KEGG pathway analysis of DEGs suggested that these DEGs might be involved in the pathogenesis and progression of CRC. In our study, the up-regulated and down-regulated DEGs were respectively enriched in both the positive and negative regulation of cell proliferation. Meanwhile, the up-regulated DEGs were involved in the apoptosis and cell cycle. A prior study confirmed that cholesterol could stimulate CRC cells proliferation, promote cell cycle progression, and inhibit cell apoptosis [23]. Another previous study also revealed that a mutation in the P53 way was closely related to the progression of CRC [24]. In our KEGG pathway results, the up-regulated DEGs were significantly enriched in the P53 pathway. Interestingly, in our research, the up-regulated DEGs were enriched in the KEGG pathway of legionellosis. However, the mechanism and relationship of the legionellosis pathway to CRC has not been studied. The role of the legionellosis pathway in CRC is worth further inquiry.

In our study, 27 hub genes were filtered out from the DEGs. The higher mRNA expression level of BIRC5, CCNB1, KIF20A, NCAPG, and TPX2 were significantly associated with the higher percentage survival among CRC patients from the TCGA. The mRNA expression levels of BIRC5, CCNB1, KIF20A, NCAPG, and TPX2 were higher in CRC samples compared with normal colorectal samples based on the TCGA and GTEx. BIRC5, CCNB1, KIF20A, NCAPG, and TPX2 were potentially involved in the occurrence and progression of CRC. The above 5 hub genes as positive prognostic indicators as they might be related to the initiation of the anti-cancer processes,

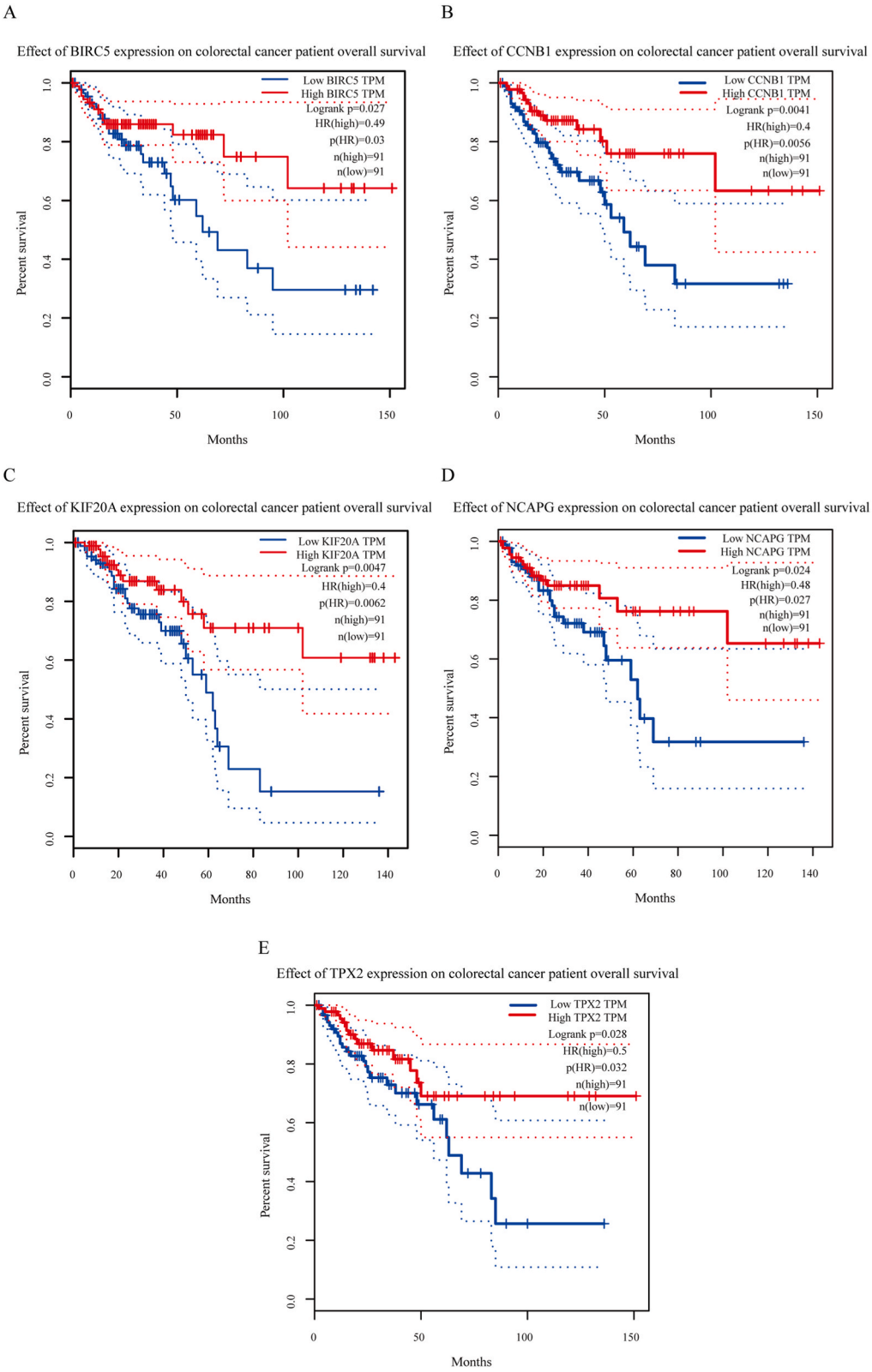

Fig. 4. The overall survival analysis of hub genes in CRC was performed through the GEPIA using clinical data of TCGA. The mRNA expression levels of BIRC5, CCNB1, KIF20A, NCAPG, and TPX2 were significantly correlated with the prognosis of CRC patients (A–E). High group: higher than the upper quartile. Low group: lower than the lower quartile. TPM: transcripts per million. The log-rank test was performed on the relevant results.

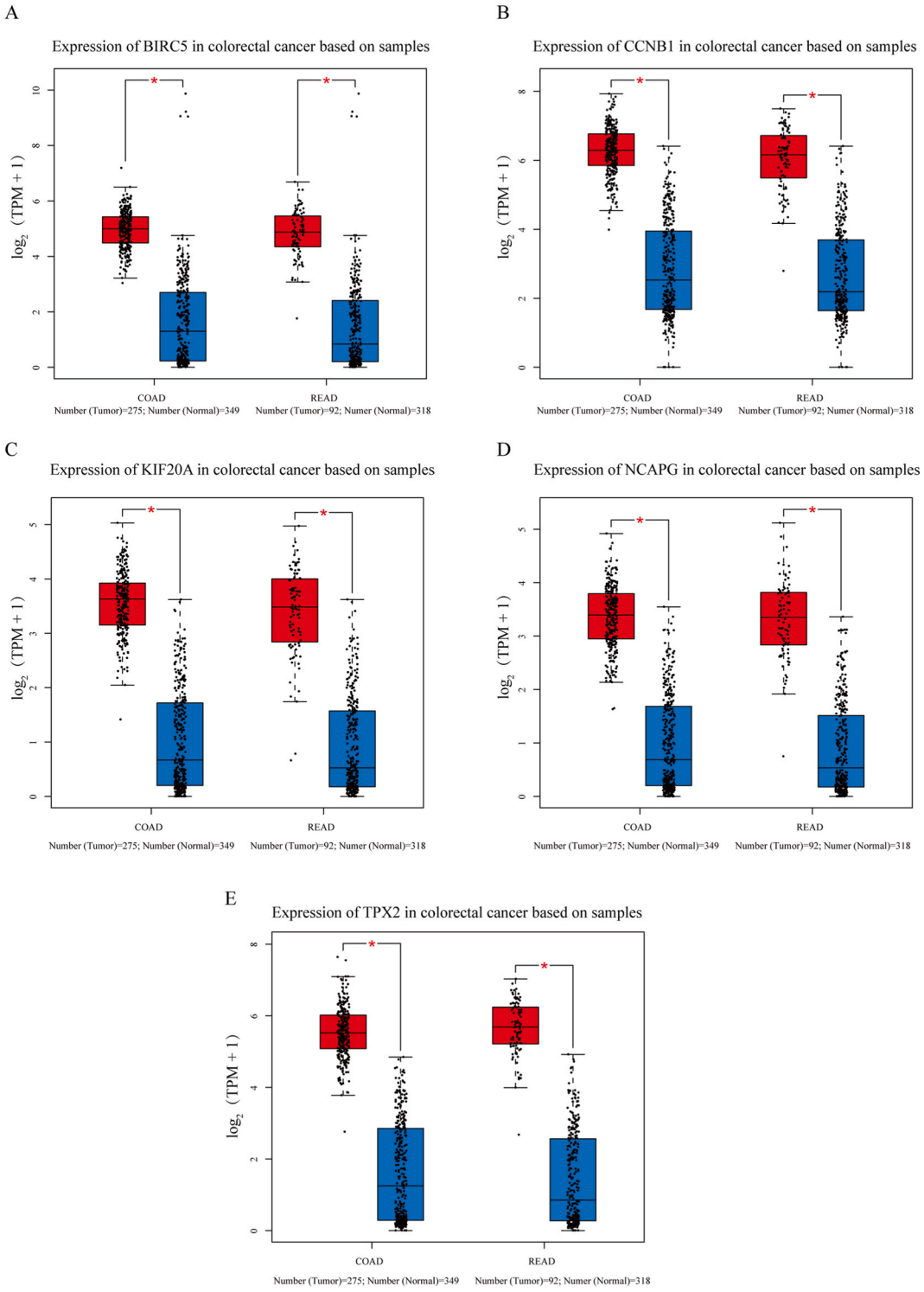

Fig. 5. The mRNA expression levels of prognostic hub genes in CRC were analyzed through the GEPIA using clinical data of TCGA and GTEx. The mRNA expression levels of BIRC5, CCNB1, KIF20A, NCAPG, and TPX2 were significantly higher in CRC samples compared with normal samples (A–E). TPM: transcripts per million. COAD: colon adenocarcinoma. READ: rectum adenocarcinoma. The *t*-test was performed on the relevant results (*P $<$ 0.05).

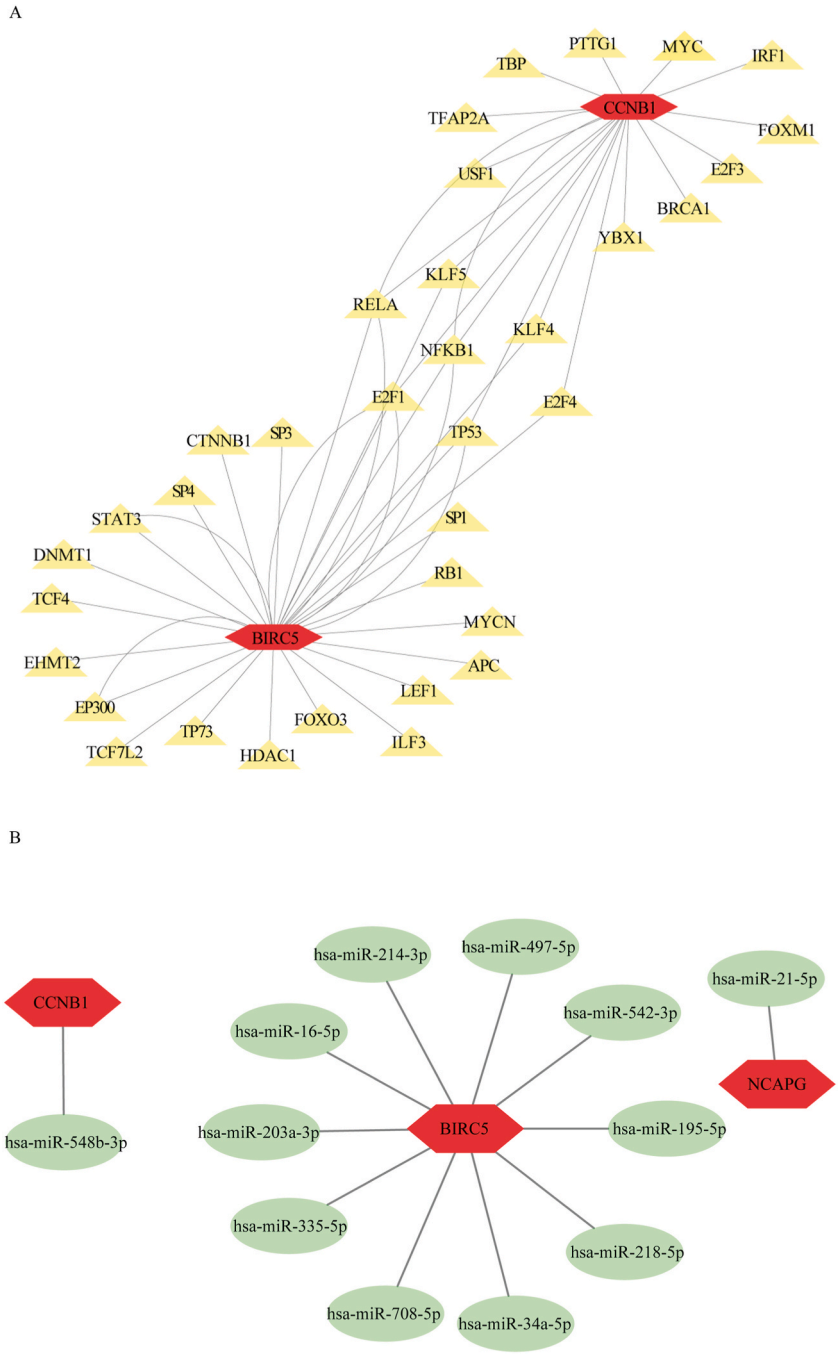

Fig. 6. The TFs-mRNA and miRNA-mRNA regulatory networks of prognostic hub genes. (A). The TFs-mRNA regulatory network was composed of 2 prognostic hub genes (CCNB1, BIRC5) and 35 TFs. (B). The miRNA-mRNA regulatory network was composed of 3 prognostic hub genes (CCNB1, BIRC5, and NCAPG) and 12 miRNAs. Red nodes represented prognostic hub genes. Yellow nodes represented TFs. Green nodes represented microRNAs. The sides represented an interaction relationship between prognostic hub genes and TFs (prognostic hub genes and miRNAs).

aggressive drug therapy, source of CRC patients, and so on.

35 TFs and 12 microRNAs were respectively screened from the TFs and miRNA-mRNA regulatory networks in our study. In a prior study, the flubendazole blocked the nuclear translocation of signal transducer and activator of transcription 3 (STAT3) in an anti-colorectal process which led to the inhibition of BIRC5 [25]. Another previous study had confirmed that KLF4 could repress the CCNB1 by promoting localized deacetylation of histone-4, which appeared to function as the tumor suppressor in gastrointestinal cancer [26]. In our TFs-mRNA regulatory network, STAT3 and KLF4 also respectively targeted the BIRC5 and CCNB1. The miR-218

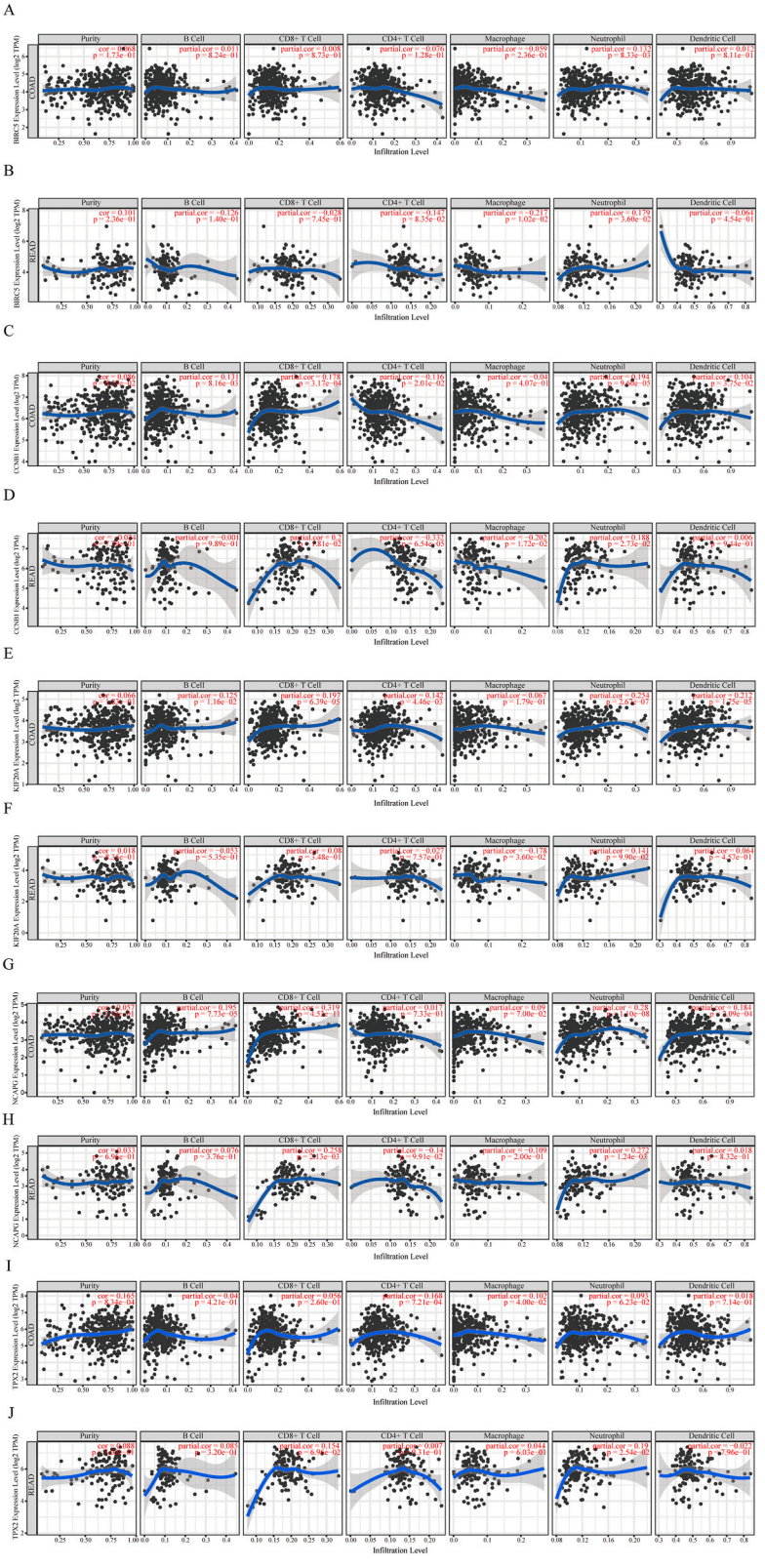

(caption on next page)

Fig. 7. The correlation between the mRNA levels of prognostic hub genes and infiltration levels of immune cells in CRC. In colon adenocarcinoma, the mRNA expression levels of BIRC5 was positively correlated with the abundance of neutrophil (A); CCNB1 was positively correlated with the abundance of B cells, $CD8^+$ T cells, neutrophils, dendritic cells and negatively correlated with $CD4^+$ T cells (C); KIF20A was positively correlated with the abundance of B cells, $CD8^+$ T cells, $CD4^+$ T cells, neutrophils, and dendritic cells (E); NCAPG was positively correlated with the abundance of B cells, $CD8^+$ T cells, neutrophils, and dendritic cells (G); TPX2 was positively correlated with the abundance of purity, $CD4^+$ T cells, and macrophage (I). In rectum adenocarcinoma, the mRNA expression levels of BIRC5 was positively correlated with the abundance of neutrophils and negatively correlated with macrophages (B); CCNB1 was positively correlated with the abundance of $CD8^+$ T cells, neutrophils and negatively correlated with $CD4^+$ T cells, and macrophage (D); KIF20A was negatively correlated with the abundance of macrophages (F); NCAPG was positively correlated with the abundance of $CD8^+$ T cells and neutrophils (H); TPX2 was positively correlated with the abundance of neutrophils (J). TPM: transcripts per million. COAD: colon adenocarcinoma. READ: rectum adenocarcinoma.

was significantly down-regulated in CRC samples and the re-expression of miR-218 inhibited CRC cell proliferation, promoted apoptosis, and arrested cell cycle by suppression [27]. A recent study suggested that miR-195–5p had a direct association with BIRC5 in CRC, which might serve as the therapeutic target [28]. These results were similar to our results on the regulation of microRNAs on BIRC5. The mechanisms of other miRNAs' regulation on the hub genes require further study.

The cyclin B1 (CCNB1) is the regulatory protein involved in mitosis and is the crucial cell cycle regulator of the G2/M checkpoint [29]. Lei et al. [30], identified that the CCNB1 was overexpressed in human CRC tissues and that COAD patients with high expression of CCNB1 had a better prognosis through the bioinformatic analysis. Our results also demonstrated the mRNA and protein levels of CCNB1 were higher in CRC tissues than normal colorectal tissues, and that the high expression of CCNB1 in CRC patients was a favorable prognostic indicator. The expression of CCNB1 was significantly positively associated with $CD8^+$ T cell and also negatively associated with $CD4^+$ T cell infiltration in CRC. The CCNB1 elicited helper T-cell dependent antibody responses in vivo [31].

The kinesin family member 20 A (KIF20A), known as the mitotic kinesin-like protein, is a member of the kinesin-6 family which is involved in spindle assembly and it interacts with mitotic regulators during mitosis [32]. Xiong et al. [33], reported that the up-regulation of KIF20A enhanced the malignant features of CRC, including proliferation, metastasis, and chemoresistance. Furthermore, the KIF20A could achieve its pro-tumor activities by activating the JAK/STAT3 signaling pathway. In our study, the KIF20A was overexpressed in the CRC tissues. The cancer cells overexpressing KIF20A could be recognized by the host immune response and hence KIF20A-derived peptides could be utilized as the immunotherapeutic agents [34]. In our results, the KIF20A was positively correlated with B cell, $CD8^+$ T cell, $CD4^+$ T cell, neutrophil, and dendritic cell infiltration in colon adenocarcinoma, and negatively correlated with macrophage infiltration in rectum adenocarcinoma.

The non-SMC condensing I complex subunit G (NCAPG) can be purified from the HeLa cell nucleus and it plays a critical role in condensin activation via regulation of ATPase activity [35,36]. Another integrated analysis showed that the NCAPG was significantly overexpressed in CRC samples, which was similar to our results [37]. Interestingly, in our study, the protein expression level of NCAPG was not significantly higher in rectum cancer tissues. The CRC patients with high expression of NCAPG had better overall survival rates. Large samples are required to validate these results. The NCAPG is involved in T cell proliferation and activation, including transcripts that encoded Ki67 [38]. In our study, the NCAPG demonstrated a strong positive correlation with $CD8^+$ T cell infiltration in CRC.

The target protein for Xenopus kinesin-like protein 2 (TPX2) is the major target required for chromatin-stimulated, augmin-mediated microtubule, spindle assembly, and its expression in cells is tightly regulated [39–42]. Due to the essential role played by TPX2 in mitosis, its elimination could prevent the proliferation of cancer cells. TPX2 knockdown induced cell cycle arrest, apoptosis, inhibition of cell proliferation, and invasion in various types of cancer cell lines [43–45]. High levels of TPX2 mRNA and protein were seen in a high percentage of squamous cell carcinoma of the lung cancer tissues, and the levels of expression were related to tumor grade, stage, and nodal status [46]. These findings are very similar to our results in CRC. Prior research suggested that the aberrant expression of TPX2 was significantly associated with unfavorable clinicopathological outcome in colon cancer, contrary to our findings that it was a favorable prognostic biomarker in CRC [47]. This may be due to the rectum cancer cases that were also included for survival analysis. The latest research had confirmed that highly significant down-regulation of STAT6, FOS, TGFBR2, ITK and up-regulation of TPX2, MPO, TYMS in treated chronic myeloid leukemia relative to normal samples led to the up-regulation of the cell cycle, DNA repair, and down-regulation of the cell cycle, chemokine, interleukin signaling, T cell antigen receptor signaling pathway and so on [48]. In our study, the TPX2 was positively correlated with $CD4^+$ T cell, macrophage, and neutrophil infiltration in CRC.

The baculoviral inhibitor of apoptosis repeat-containing 5 (BIRC5), frequently termed "survivin", is the smallest but most functional and complex member of the inhibitor of apoptosis protein (IAP) family [49]. The BIRC5 is almost ubiquitously expressed in human stem cells during embryogenesis and is essential for proper fetal development. However, its expression in adult tissues is tightly restricted [50]. BIRC5 was originally identified and characterized in human cancer. Generally, it is highly expressed in different kinds of cancers such as brain tumors, lung, breast, pancreatic, osteosarcoma, and cervical cancers [51]. In CRC patients, the expression levels of BIRC5 was associated with unfavorable outcomes and dwarfed survival. It could reduce tumor cell apoptosis in vivo [52]. Kimet al. [53], reported that BIRC5 was a new target gene of the T-cell factor (TCF)/β-catenin signaling axis, and the coupling increased cell proliferation to enhance cell survival in intestinal crypt cells. This pathway consisted of the presence of three TCF-binding elements (TBE) sites in the BIRC5 promoters which were directly involved in gene expression, the absolute dependence upon TCF signaling for BIRC5 expression in the embryonic intestine in vivo, and the complete resistance to apoptosis afforded by TCF-dependent expression of BIRC5. Our bioinformatics analysis had shown that the mRNA and protein expression levels of BIRC5 were higher in CRC tissues compared with normal colorectal tissues. Patients with colon adenocarcinoma and rectum adenocarcinoma, the higher expression levels of BIRC5 was associated with higher overall survival rates. Subsequently, our qPCR and

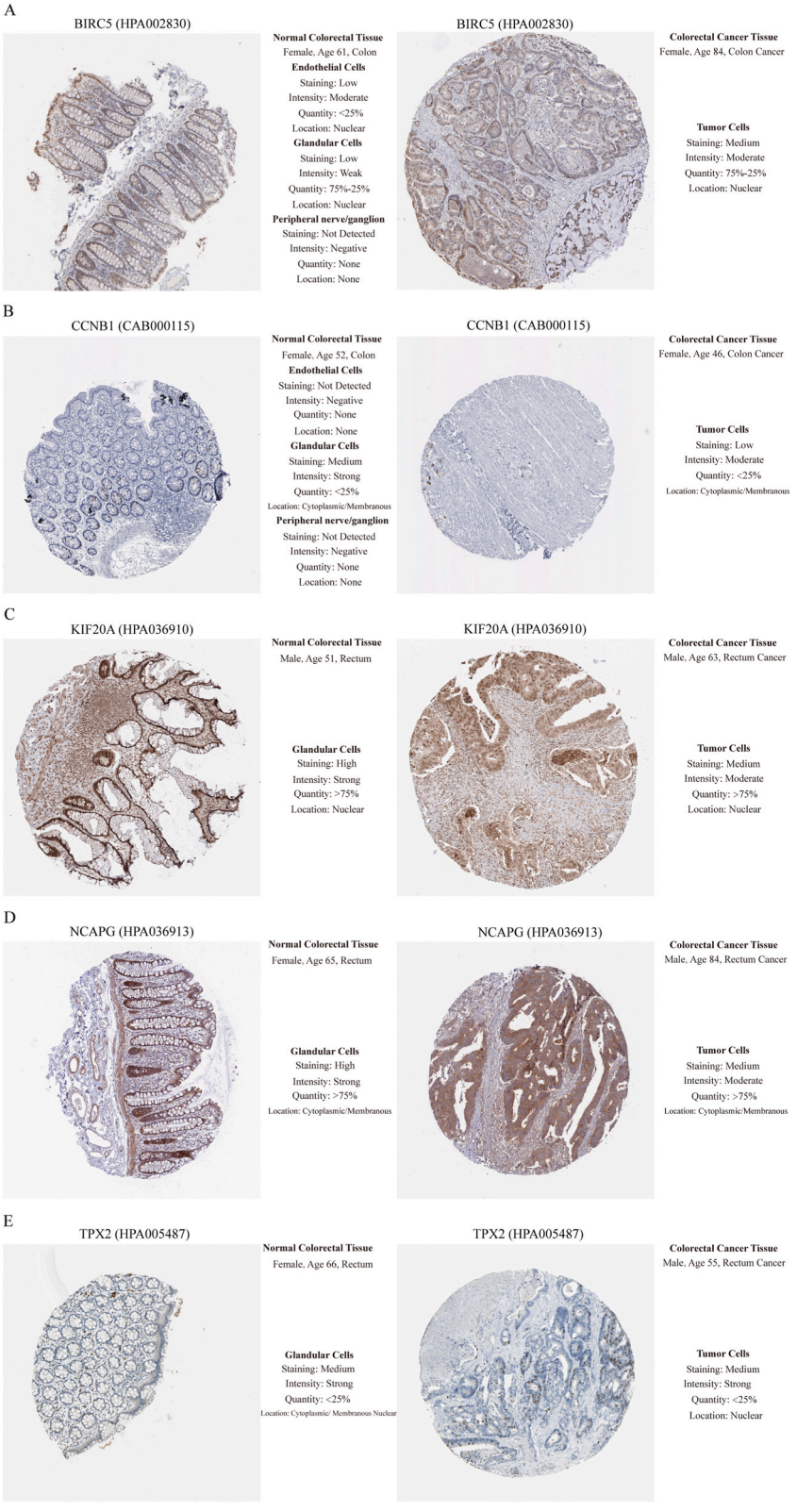

(caption on next page)

Fig. 8. The immunohistochemistry (IHC) of prognostic hub genes in the Human Protein Atlas (HPA). (A) Protein levels of BIRC5 in normal colorectal tissues and CRC tissues. (B) Protein levels of CCNB1 in normal colorectal tissues and CRC tissues. (C) Protein levels of KIF20A in normal colorectal tissues and CRC tissues. (D) Protein levels of NCAPG in normal colorectal tissues and CRC tissues. (E) Protein levels of TPX2 in normal colorectal tissues and CRC tissues.

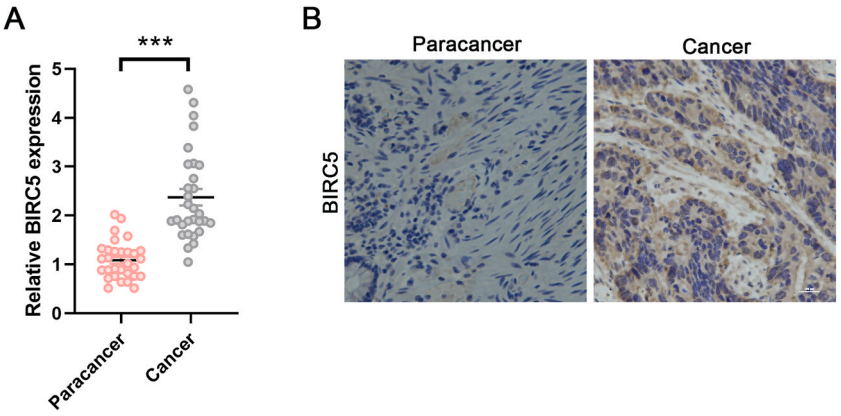

Fig. 9. BIRC5 was highly expressed in CRC tissues. (A) The mRNA levels of BIRC5 in cancer and paracancer tissues was detected by RT-PCR. (B) Expression of BIRC5 in cancer and paracancer tissues examined by immunohistochemistry. ***P $<$ 0.001 were compared to paracancer tissues.

immunohistochemical results suggested that the mRNA and protein expression levels of BIRC5 were highly expressed in CRC tissues and cells compared with normal colorectal tissues and colonic mucosal epithelial cells. In the previous study, cell free BIRC5 mRNA levels were significantly increased in serum of CRC, and significantly correlated with tumor differentiation, regional lymph node metastasis, and TNM stage [54]. BIRC5 was the promising biomarker for the prognosis of CRC.

We confirmed that down-regulation of BIRC5 expression could suppresses the proliferation, migration, and invasion of CRC cells *in vitro*. Wang et al. [55], reported that epigenetic silencing of BIRC5 could inhibit the proliferation of laryngeal squamous cell carcinoma cells and control cell cycle progression and apoptosis *in vitro*. We hypothesized that BIRC5 might act as an oncogene of CRC development and progression. In our study, the expression of BIRC5 was significantly positively correlated with neutrophil infiltration in colon adenocarcinoma and rectum adenocarcinoma, and negatively correlated with macrophage infiltration in rectum adenocarcinoma. It was reported that clear cell renal cell carcinoma expressing high levels of BIRC5 and PDL1 exhibited the increased infiltration by mononuclear cells, including-specific $CD8^+$ T cells. The BIRC5 and PDL1 collaborated as the predictors of adverse clear cell renal cell carcinoma behavior and might also work through immunological mechanisms to worsen progression and outcome [56]. We hypothesized that BIRC5 might be involved in the progression of CRC through the regulation of immune cells. The mechanisms of BIRC5 in CRC are worth further experimentations.

The major deficiency of our research was that our analysis was bioinformatics exploration and cytological experiments. Therefore, zoological experiments, and drug trials are urgently needed to verify our results. Our results might provide valuable information and pathways concerned with CRC for better clarifying the molecular mechanism of CRC carcinogenesis.

5. Conclusion

In conclusion, 281 DEGs were identified in CRC. Their enrichment of GO term and KEGG pathways were closely associated with the occurrence and development of CRC. Among the 27 hub genes, BIRC5, CCNB1, KIF20A, NCAPG, and TPX2 might be promising biomarkers for prognosis in CRC. These hub genes were closely associated with transcription factors, microRNAs, and immune infiltration, which might be involved in the regulation of CRC. BIRC5 highly expressed in CRC tissues and cells, and promoted the proliferation, migration, and invasion of CRC cells *in vitro*. BIRC5 plays an important role in the development and progression of CRC. These findings can be helpful for prognosis, and targeted therapy on CRC.

Ethical approval

Ethical approval was obtained for all experimental procedures by the Ethical Committee of Fifth Affiliated Hospital of Southern Medical University, Guangzhou, China.

Statement of human and animals rights

The assays on human subjects were carried out in accordance with Declaration of Helsinki.

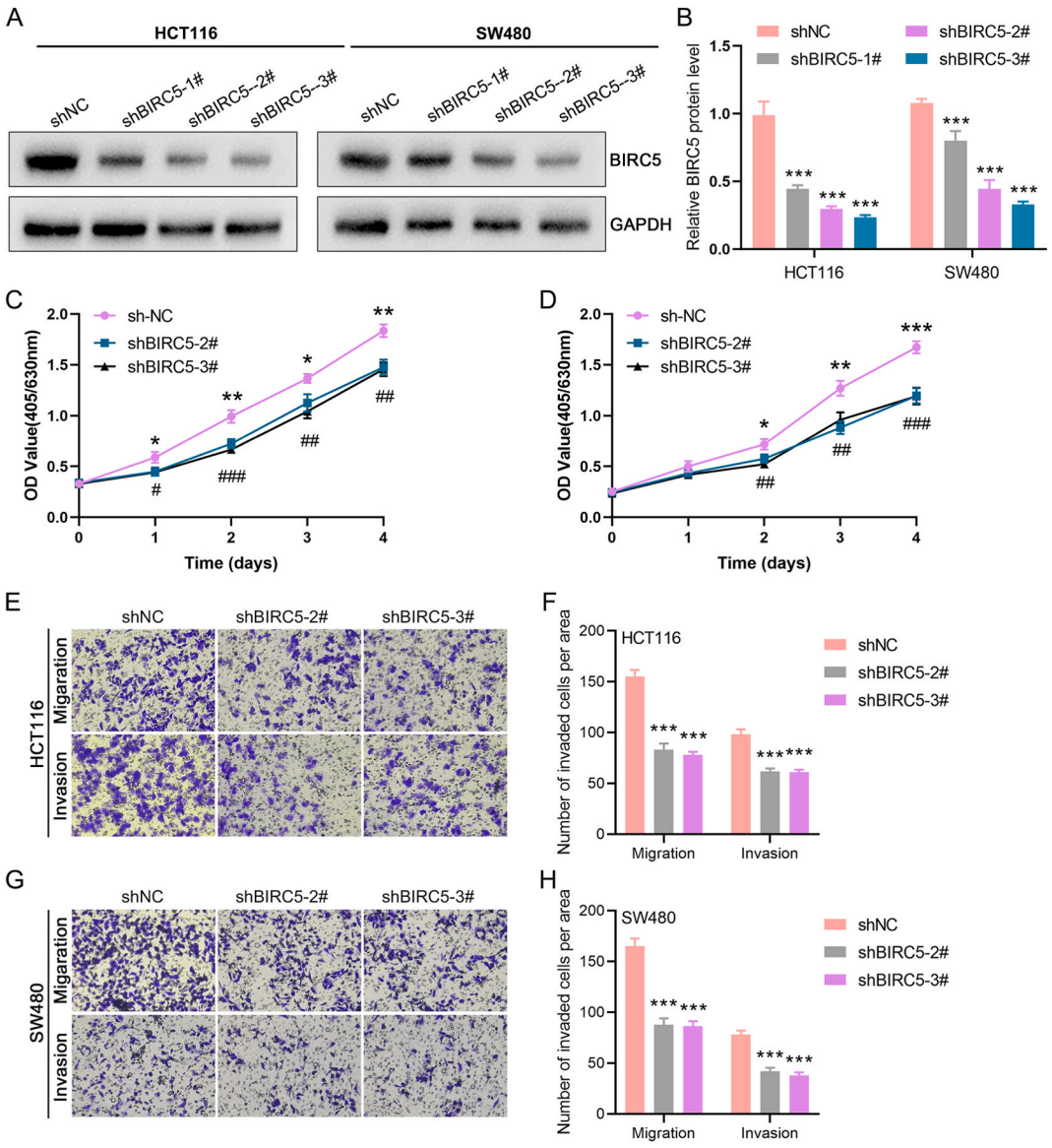

Fig. 10. Down-regulation of BIRC5 inhibited proliferation, migration and invasion of CRC cells. (A) Western blotting showed that the expression of BIRC5 was down-regulated by shRNA lentiviral particles transduction. (B) BIRC5 expression was significantly decreased in the colorectal cancer cells transfected with BIRC5 shRNA, compared with scrambled shRNA. (*C*–D) CCK8 assay showed that knockdown of BIRC5 inhibited cell proliferation of HCT116 and SW480 cells. (*E*–F) Transwell assay showed migration and invasion in HCT116 cell line stably expressing BIRC5 shRNA. (G–H) Transwell assay showed migration and invasion in SW480 cell line stably expressing BIRC5 shRNA. *P < 0.05, **P < 0.01 and ***P < 0.001 were compared to shNC group. #P < 0.05, ##P < 0.01 and ###P < 0.001 were compared to shNC group.

Statement of informed consent

Written informed consent was obtained from their anonymized information to be published in this article.

Authors' contribution

Baolong Li: Conceived and designed the experiments.
Min Guo; Xiaxi Li: Performed the experiments; Contributed reagents, materials, analysis tools; Wrote the paper.
Jiong Li: Analyzed and interpreted the data.

Availability of data and materials

The datasets used and/or analyzed during the current study are available from the corresponding author. The datasets analyzed in the study could be found in GEO (https://www.ncbi.nlm.gov/geo) and TCGA (https://portal.gdc.cancer.gov/).

Declaration of competing interest

The authors declare that they have no known competing financial interests or personal relationships that could have appeared to influence the work reported in this paper.

References

[1] F. Bray, J. Ferlay, I. Soerjomataram, R.L. Siegel, L.A. Torre, A. Jemal, Global cancer statistics 2018: GLOBOCAN estimates of incidence and mortality worldwide for 36 cancers in 185 countries, CA A Cancer J. Clin. 68 (6) (2018) 394–424.

[2] R.L. Siegel, K.D. Miller, A. Goding Sauer, S.A. Fedewa, L.F. Butterly, J.C. Anderson, A. Cercek, R.A. Smith, A. Jemal, Colorectal cancer statistics, 2020, CA A Cancer J. Clin. 70 (3) (2020) 145–164.

[3] M. Arnold, M.S. Sierra, M. Laversanne, I. Soerjomataram, A. Jemal, F. Bray, Global patterns and trends in colorectal cancer incidence and mortality, Gut 66 (4) (2017) 683–691.

[4] N. Keum, E. Giovannucci, Global burden of colorectal cancer: emerging trends, risk factors and prevention strategies, Nat. Rev. Gastroenterol. Hepatol. 16 (12) (2019) 713–732.

[5] K.W. Jasperson, T.M. Tuohy, D.W. Neklason, R.W. Burt, Hereditary and familial colon cancer, Gastroenterology 138 (6) (2010) 2044–2058.

[6] A.C. Anderson, N. Joller, V.K. Kuchroo, Lag-3, tim-3, and TIGIT: Co-inhibitory receptors with specialized functions in immune regulation, Immunity 44 (5) (2016) 989–1004.

[7] C.S. Grasso, M. Giannakis, D.K. Wells, T. Hamada, X.J. Mu, M. Quist, J.A. Nowak, R. Nishihara, Z.R. Qian, K. Inamura, et al., Genetic mechanisms of immune evasion in colorectal cancer, Cancer Discov. 8 (6) (2018) 730–749.

[8] Y. Wang, L. Li, J.D. Cohen, I. Kinde, J. Ptak, M. Popoli, J. Schaefer, N. Silliman, L. Dobbyn, J. Tie, et al., Prognostic potential of circulating tumor DNA measurement in postoperative surveillance of nonmetastatic colorectal cancer, JAMA Oncol. 5 (8) (2019) 1118–1123.

[9] Y. Lu, X. Zhao, Q. Liu, C. Li, R. Graves-Deal, Z. Cao, B. Singh, J.L. Franklin, J. Wang, H. Hu, et al., lncRNA MIR100HG-derived miR-100 and miR-125b mediate cetuximab resistance via Wnt/β-catenin signaling, Nat. Med. 23 (11) (2017) 1331–1341.

[10] S. Uddin, M. Ahmed, A. Hussain, J. Abubaker, N. Al-Sanea, A. AbdulJabbar, L.H. Ashari, S. Alhomoud, F. Al-Dayel, Z. Jehan, et al., Genome-wide expression analysis of Middle Eastern colorectal cancer reveals FOXM1 as a novel target for cancer therapy, Am. J. Pathol. 178 (2) (2011) 537–547.

[11] P. Alhopuro, H. Sammalkorpi, I. Niittymäki, M. Biström, A. Raitila, J. Saharinen, K. Nousiainen, H.J. Lehtonen, E. Heliövaara, J. Puhakka, et al., Candidate driver genes in microsatellite-unstable colorectal cancer, Int. J. Cancer 130 (7) (2012) 1558–1566.

[12] J.M. Sayagués, L.A. Corchete, M.L. Gutiérrez, M.E. Sarasquete, M. Del Mar Abad, O. Bengoechea, E. Fermiñán, M.F. Anduaga, S. Del Carmen, M. Iglesias, et al., Genomic characterization of liver metastases from colorectal cancer patients, Oncotarget 7 (45) (2016) 72908–72922.

[13] da W. Huang, B.T. Sherman, R.A. Lempicki, Systematic and integrative analysis of large gene lists using DAVID bioinformatics resources, Nat. Protoc. 4 (1) (2009) 44–57.

[14] da W. Huang, B.T. Sherman, R.A. Lempicki, Bioinformatics enrichment tools: paths toward the comprehensive functional analysis of large gene lists, Nucleic Acids Res. 37 (1) (2009) 1–13.

[15] D. Szklarczyk, J.H. Morris, H. Cook, M. Kuhn, S. Wyder, M. Simonovic, A. Santos, N.T. Doncheva, A. Roth, P. Bork, et al., The STRING database in 2017: quality-controlled protein-protein association networks, made broadly accessible, Nucleic Acids Res. 45 (D1) (2017) D362–D368.

[16] G.D. Bader, C.W. Hogue, An automated method for finding molecular complexes in large protein interaction networks, BMC Bioinf. 4 (2003) 2.

[17] Z. Tang, C. Li, B. Kang, G. Gao, C. Li, Z. Zhang, GEPIA: a web server for cancer and normal gene expression profiling and interactive analyses, Nucleic Acids Res. 45 (W1) (2017 Jul 3) W98–W102, https://doi.org/10.1093/nar/gkx247. PMID: 28407145; PMCID: PMC5570223.

[18] Y. Fan, K. Siklenka, S.K. Arora, P. Ribeiro, S. Kimmins, J. Xia, miRNet - dissecting miRNA-target interactions and functional associations through network-based visual analysis, Nucleic Acids Res. 44 (W1) (2016) W135–W141.

[19] H.Y. Huang, Y.C. Lin, J. Li, K.Y. Huang, S. Shrestha, H.C. Hong, Y. Tang, Y.G. Chen, C.N. Jin, Y. Yu, et al., miRTarBase 2020: updates to the experimentally validated microRNA-target interaction database, Nucleic Acids Res. 48 (D1) (2020) D148–D154.

[20] T. Li, J. Fan, B. Wang, N. Traugh, Q. Chen, J.S. Liu, B. Li, X.S. Liu, TIMER: a web server for comprehensive analysis of tumor-infiltrating immune cells, Cancer Res. 77 (21) (2017) e108–e110.

[21] A. Asplund, P.H. Edqvist, J.M. Schwenk, F. Pontén, Antibodies for profiling the human proteome-The Human Protein Atlas as a resource for cancer research, Proteomics 12 (13) (2012) 2067–2077.

[22] E. Dekker, P.J. Tanis, J.L.A. Vleugels, P.M. Kasi, M.B. Wallace, Colorectal cancer, Lancet 394 (10207) (2019) 1467–1480.

[23] Y. Wang, C. Liu, L. Hu, Cholesterol regulates cell proliferation and apoptosis of colorectal cancer by modulating miR-33a-PIM3 pathway, Biochem. Biophys. Res. Commun. 511 (3) (2019) 685–692.

[24] E.J. Kuipers, W.M. Grady, D. Lieberman, T. Seufferlein, J.J. Sung, P.G. Boelens, C.J. van de Velde, T. Watanabe, Colorectal cancer, Nat. Rev. Dis. Prim. 1 (2015), 15065.

[25] S. Lin, L. Yang, Y. Yao, L. Xu, Y. Xiang, H. Zhao, L. Wang, Z. Zuo, X. Huang, C. Zhao, Flubendazole demonstrates valid antitumor effects by inhibiting STAT3 and activating autophagy, J. Exp. Clin. Cancer Res. 38 (1) (2019) 293.

[26] P.M. Evans, W. Zhang, X. Chen, J. Yang, K.K. Bhakat, C. Liu, Kruppel-like factor 4 is acetylated by p300 and regulates gene transcription via modulation of histone acetylation, J. Biol. Chem. 282 (47) (2007) 33994–34002.

[27] P.L. Li, X. Zhang, L.L. Wang, L.T. Du, Y.M. Yang, J. Li, C.X. Wang, MicroRNA-218 is a prognostic indicator in colorectal cancer and enhances 5-fluorouracil-induced apoptosis by targeting BIRC5, Carcinogenesis 36 (12) (2015) 1484–1493.

[28] M.L. Slattery, L.E. Mullany, L.C. Sakoda, R.K. Wolff, W.S. Samowitz, J.S. Herrick, Dysregulated genes and miRNAs in the apoptosis pathway in colorectal cancer patients, Apoptosis 23 (3–4) (2018) 237–250.

[29] J. Liu, Y. Wen, Z. Liu, S. Liu, P. Xu, Y. Xu, S. Deng, S. Hu, R. Luo, J. Jiang, et al., VPS33B modulates c-Myc/p53/miR-192-3p to target CCNB1 suppressing the growth of non-small cell lung cancer, Mol. Ther. Nucleic Acids 23 (2020) 324–335.

[30] X. Lei, J. Jing, M. Zhang, B. Guan, Z. Dong, C. Wang, Bioinformatic identification of hub genes and analysis of prognostic values in colorectal cancer, Nutr. Cancer 73 (11–12) (2021) 2568–2578.

[31] H. Suzuki, D.F. Graziano, J. McKolanis, O.J. Finn, T cell-dependent antibody responses against aberrantly expressed cyclin B1 protein in patients with cancer and premalignant disease, Clin. Cancer Res. 11 (4) (2005) 1521–1526.

[32] J.M. Cesario, J.K. Jang, B. Redding, N. Shah, T. Rahman, K.S. McKim, Kinesin 6 family member Subito participates in mitotic spindle assembly and interacts with mitotic regulators, J. Cell Sci. 119 (Pt 22) (2006) 4770–4780.

[33] M. Xiong, K. Zhuang, Y. Luo, Q. Lai, X. Luo, Y. Fang, Y. Zhang, A. Li, S. Liu, KIF20A promotes cellular malignant behavior and enhances resistance to chemotherapy in colorectal cancer through regulation of the JAK/STAT3 signaling pathway, Aging (Albany NY) 11 (24) (2019) 11905–11921.

[34] F. Xie, C. He, S. Gao, Z. Yang, L. Li, L. Qiao, L. Fang, KIF20A silence inhibits the migration, invasion and proliferation of non-small cell lung cancer and regulates the JNK pathway, Clin. Exp. Pharmacol. Physiol. 47 (1) (2020) 135–142.
[35] A. Lammens, A. Schele, K.P. Hopfner, Structural biochemistry of ATP-driven dimerization and DNA-stimulated activation of SMC ATPases, Curr. Biol. 14 (19) (2004) 1778–1782.
[36] R. Palou, T. Dhanaraman, R. Marrakchi, M. Pascariu, M. Tyers, D. D'Amours, Condensin ATPase motifs contribute differentially to the maintenance of chromosome morphology and genome stability, PLoS Biol. 16 (6) (2018), e2003980.
[37] X. Ding, H. Duan, H. Luo, Identification of core gene expression signature and key pathways in colorectal cancer, Front. Genet. 11 (2020) 45.
[38] T. Bradley, M. Kuraoka, C.H. Yeh, M. Tian, H. Chen, D.W. Cain, X. Chen, C. Cheng, A.H. Ellebedy, R. Parks, et al., Immune checkpoint modulation enhances HIV-1 antibody induction, Nat. Commun. 11 (1) (2020) 948.
[39] S. Petry, A.C. Groen, K. Ishihara, T.J. Mitchison, R.D. Vale, Branching microtubule nucleation in Xenopus egg extracts mediated by augmin and TPX2, Cell 152 (4) (2013) 768–777.
[40] T. Wittmann, M. Wilm, E. Karsenti, I. Vernos, TPX2, A novel xenopus MAP involved in spindle pole organization, J. Cell Biol. 149 (7) (2000) 1405–1418.
[41] O.J. Gruss, R.E. Carazo-Salas, C.A. Schatz, G. Guarguaglini, J. Kast, M. Wilm, N. Le Bot, I. Vernos, E. Karsenti, I.W. Mattaj, Ran induces spindle assembly by reversing the inhibitory effect of importin alpha on TPX2 activity, Cell 104 (1) (2001) 83–93.
[42] O.J. Gruss, M. Wittmann, H. Yokoyama, R. Pepperkok, T. Kufer, H. Silljé, E. Karsenti, I.W. Mattaj, I. Vernos, Chromosome-induced microtubule assembly mediated by TPX2 is required for spindle formation in HeLa cells, Nat. Cell Biol. 4 (11) (2002) 871–879.
[43] P. Vainio, J.P. Mpindi, P. Kohonen, V. Fey, T. Mirtti, K.A. Alanen, M. Perälä, O. Kallioniemi, K. Iljin, High-throughput transcriptomic and RNAi analysis identifies AIM1, ERGIC1, TMED3 and TPX2 as potential drug targets in prostate cancer, PLoS One 7 (6) (2012), e39801.
[44] S.L. Warner, B.J. Stephens, S. Nwokenkwo, G. Hostetter, A. Sugeng, M. Hidalgo, J.M. Trent, H. Han, D.D. Von Hoff, Validation of TPX2 as a potential therapeutic target in pancreatic cancer cells, Clin. Cancer Res. 15 (21) (2009) 6519–6528.
[45] R. Satow, M. Shitashige, Y. Kanai, F. Takeshita, H. Ojima, T. Jigami, K. Honda, T. Kosuge, T. Ochiya, S. Hirohashi, et al., Combined functional genome survey of therapeutic targets for hepatocellular carcinoma, Clin. Cancer Res. 16 (9) (2010) 2518–2528.
[46] L.T. Smith, J. Mayerson, N.J. Nowak, D. Suster, N. Mohammed, S. Long, H. Auer, S. Jones, C. McKeegan, G. Young, et al., 1 amplification in giant-cell tumor of bone: array CGH, FISH, and association with outcome, Genes Chromosomes Cancer 45 (10) (2006) 957–966.
[47] P. Wei, N. Zhang, Y. Xu, X. Li, D. Shi, Y. Wang, D. Li, S. Cai, TPX2 is a novel prognostic marker for the growth and metastasis of colon cancer, J. Transl. Med. 11 (2013) 313.
[48] N. Singh, A.K. Tripathi, D.K. Sahu, A. Mishra, M. Linan, B. Argente, J. Varkey, N. Parida, R. Chowdhry, H. Shyam, et al., Differential genomics and transcriptomics between tyrosine kinase inhibitor-sensitive and -resistant BCR-ABL-dependent chronic myeloid leukemia, Oncotarget 9 (54) (2018) 30385–30418.
[49] D.C. Altieri, Survivin - the inconvenient IAP, Semin. Cell Dev. Biol. 39 (2015) 91–96.
[50] G. Ambrosini, C. Adida, D.C. Altieri, A novel anti-apoptosis gene, survivin, expressed in cancer and lymphoma, Nat. Med. 3 (8) (1997) 917–921.
[51] S. Fukuda, L.M. Pelus, Survivin, a cancer target with an emerging role in normal adult tissues, Mol. Cancer Therapeut. 5 (5) (2006) 1087–1098.
[52] A.I. Sarela, N. Scott, J. Ramsdale, A.F. Markham, P.J. Guillou, Immunohistochemical detection of the anti-apoptosis protein, survivin, predicts survival after curative resection of stage II colorectal carcinomas, Ann. Surg Oncol. 8 (4) (2001) 305–310.
[53] P.J. Kim, J. Plescia, H. Clevers, E.R. Fearon, D.C. Altieri, Survivin and molecular pathogenesis of colorectal cancer, Lancet 362 (9379) (2003) 205–209.
[54] H. Wang, X. Zhang, L. Wang, G. Zheng, L. Du, Y. Yang, Z. Dong, Y. Liu, A. Qu, C. Wang, Investigation of cell free BIRC5 mRNA as a serum diagnostic and prognostic biomarker for colorectal cancer, J. Surg. Oncol. 109 (6) (2014) 574–579.
[55] N. Wang, X. Huang, J. Cheng, BIRC5 promotes cancer progression and predicts prognosis in laryngeal squamous cell carcinoma, PeerJ 10 (2022), e12871.
[56] A.E. Krambeck, H. Dong, R.H. Thompson, S.M. Kuntz, C.M. Lohse, B.C. Leibovich, M.L. Blute, T.J. Sebo, J.C. Cheville, A.S. Parker, et al., Survivin and b7-h1 are collaborative predictors of survival and represent potential therapeutic targets for patients with renal cell carcinoma, Clin. Cancer Res. 13 (6) (2007) 1749–1756.